Radiation and meteorology at Ice Station Belgica, October 2007, Bellingshausen Sea, Antarctica.

Martin Vancoppenolle
Institut d'Astronomie et de Géophyisique Georges Lemaître
Université de Louvain, Louvain-la-Neuve, Belgique

1. Ship track and ice station

3 Way-in stations were performed on JD 268, 269, 270. Then, the RVIB N.B. Palmer remained on station (Ice Station Belgica, ISB) from Sep 28th (JD 271) to Oct 23rd (JD 296) and drifted in an area situated between 69 and 71 °S and 90 and 95°E. The drift was initially very intense to the East due to a strong storm with maximum wind speeds around 30 m/s. From JD 277 to 285, the drift was to the west, and finally turned back to the east until the end of the station. Science was done at the Belgian Biogeochemistry (BB) sites on ISB from JD 274 to 296.

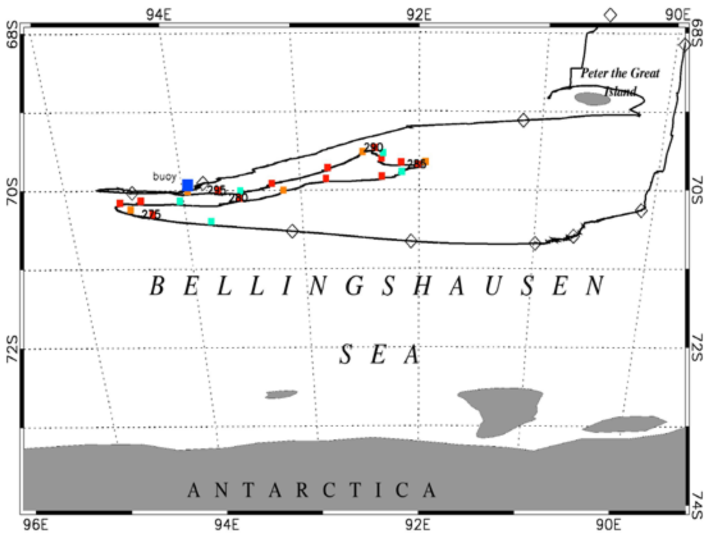

Fig. 1: NB Palmer's track in the Bellingshausen Sea. Symbols indicate ship position every day. Colored symbols indicate science days at the Ice Station Belgica. JD is written every five days. Blue (orange) squares indicate visits at the Brussels (Liège) site.

Two sites were deployed. The first (Brussels) had ice thickness typically around 60 cm and thin snow (less than 10 cm). The second site had thicker ice, typically around 120 cm and deeper snow (more than 30 cm).

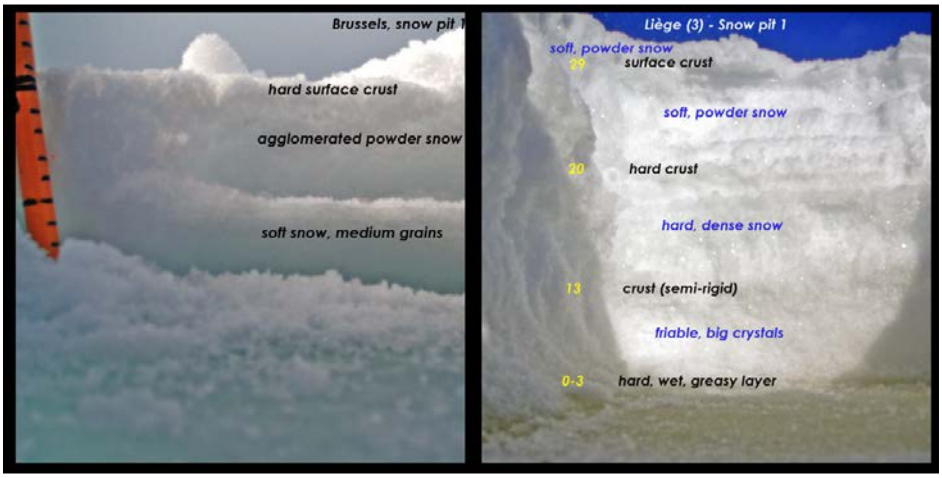

Fig. 2: Snow pits made at Brussels (left, visit #4) and at Liège (right, visit #3).

2. Data collections

The first data set consists of ship-based observations (**SHIP**) of wind, temperature, relative humidity and radiation. The thermometer and hygrometer stand at a height of 15 m relative to sea level. The barometer is at 30 m. The anemometer, as well as the radiometers are at 30.5 m. Radiometers include a pyranometer (SW), a pyrgeometer (LW), and a PAR radiometer. Longwave radiation (F_{LW}, W.m^{-2}) spans the 4-50 µm spectrum, while the incoming solar radiation (F_{SW}, W.m^{-2}) spans the 0.3 to 3.0 µm range (close UV, visible and near IR). PAR (photosynthetically absorbed radiation) covers the 350-700 nm range. Data cover JD 266-301.

The second data set consists of measurements made in situ (**INSITU**). First, a meteorological tower including a wind vane, a thermometer and an hygrometer was set at Brussels site by K. Johnson and G. Carnat. Data cover JD 275-295. Second, a series of F_{SW} measurements made with a portable pyranometer were made.

A third data set (**VISUAL**) includes 282 hourly visual observations of cloudiness and snowfall made mostly during daylight hours, covering 52% of the total drift station time. Data cover JD 276-296.

The last data (**BB**) set consists in measurements of snow depth and albedo made at both BB sites. Data include 5 visits at both sites over JD 274-296.

3. Meteorology

3.1 Instruments comparison

Fig. 2 shows the compared values of SHIP and TOWER wind and temperature observations. First, the SHIP wind speed on average 1.7 times higher than TOWER. The difference between both is proportional to the wind speed. The quite stable over time friction velocity u*=0.72 m/s found by computing u*= (kz) Δu / Δz, where k =0.4 is the Von Karman constant suggests that this is due to the difference in altitude of the anemometers in the surface layer. Second, the SHIP temperature is always higher than the TOWER value, by 1°C on average. There is a tendency of the temperature difference between sensors to decrease toward warm temperatures. Nevertheless, this tendency is not clear enough to reject a potential warming ship effect.

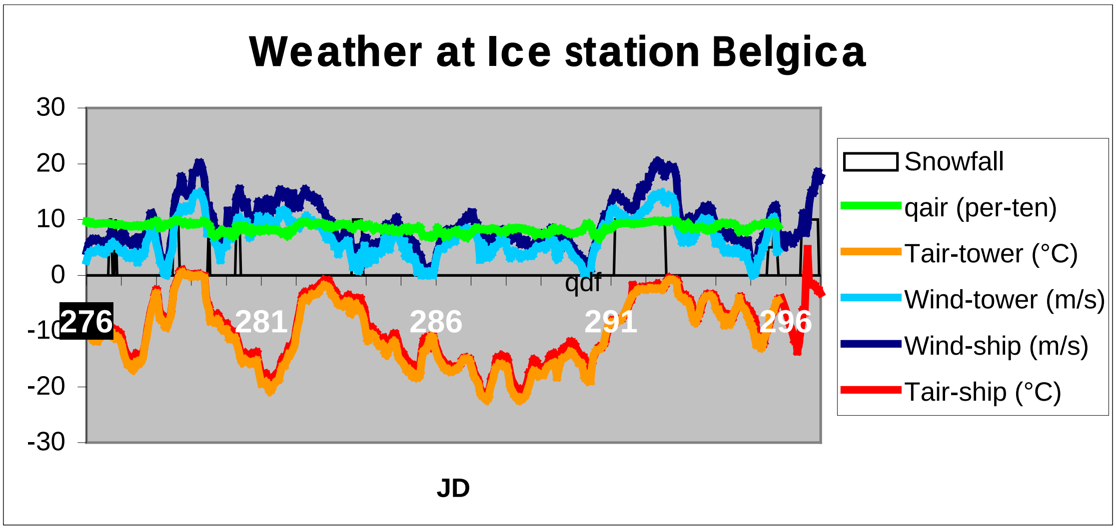

Fig. 3: Wind, temperature from SHIP and TOWER data sets recorded during ISB (blue and red curves). VISUAL Snow fall index (0 : no snow falling, 1: snow falling) is also plotted. Finally, the TOWER relative humidity (in 10ths) is also drawn.

The SHIP hygrometer was not functionning during most of the cruise. Nevertheless, the intercomparison between SHIP and TOWER instruments, from JD 292-296 after the SHIP hygrometer was repaired shows very little, non systematic difference (0-2%).

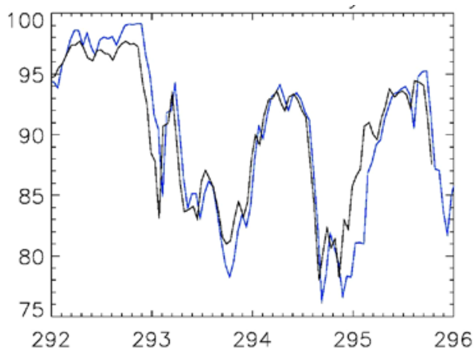

Fig. 4 : Relative humidity recorded by the SHIP (dark) and the TOWER (light) hygrometers between JD 292 and 296.

3.2 Meteo at Ice Station Belgica

The weather at Ice Station Belgica was characterized by typical spring conditions. Air temperature was on average -9.5°C, winds were on average blowing at 8.9 m/s with maxima at 20 m/s while the mean humidity was 85%. The weather variability seemed to mostly be driven by the wind direction and the continental / oceanic origin of air masses. When the winds were blowing from the North, warm (from -5 to 0 °C) and wet (relative humidity from 90 to 100%) oceanic air was advected on our floe. When the wind blew from the South, cold (from -20 to -10°C) and dry (70-85¨%) continental air was brought to the station. Intermediate regimes were found when winds blew from other directions. 9 snowfall events were counted visually, and 3 were noted as heavy on JD 283, 291-292 and 295-296. Clear skies were present mostly under dry and cold weather conditions. Average cloudiness from visual observations was 4.7, and there were 48 % of cloudy sky hours. Sky is supposed cloudy if the visual cloudiness is higher than 3. This suggests that both information (cloudiness and cloud hours) are practically equivalent at sufficiently long long time scales. Reconstructed cloudiness from the anomalies of radiative fluxes is equal to 5.7, and also covers night time. We will come back to cloudiness reconstruction later on.

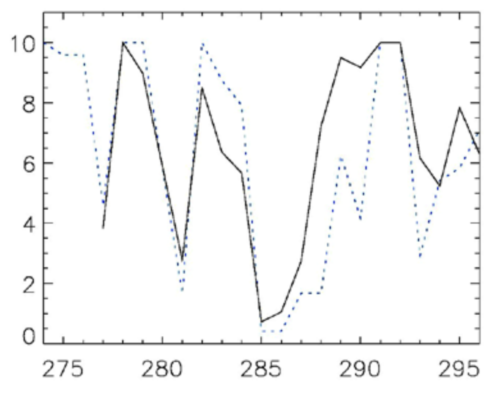

Fig. 5: Daily cloudiness (tenths) from interpolated, daily-averaged visual observations (solid) and from a reconstruction using hourly anomalies of radiative fluxes (dotted). X axis refers to JD.

4. Radiation

4.1 Pyranometers intercalibration

In situ and ship-based levels of shortwave SW radiation show significant differences. Both records have their advantages. The INSITU is expected to be more adapted to actual ice conditions, while SHIP has a continuous 1-min resolution record. The differences come either (1) from the radiometers themselves or (2) from difference in height (3) from differences in local weather conditions. To address (1), a direct intercalibration exercise was performed. It consisted in hanging the INSITU portable radiometer, just next to the SHIP pyranometer, on the top of the ship's mast, over a 15-min period and taking observation at a rate of 1 obs. per minute (see Fig. 1). The conclusion of that climbing adventure is that pyranometers can be considered as equivalent (Av. err.=0.34 W/m²).

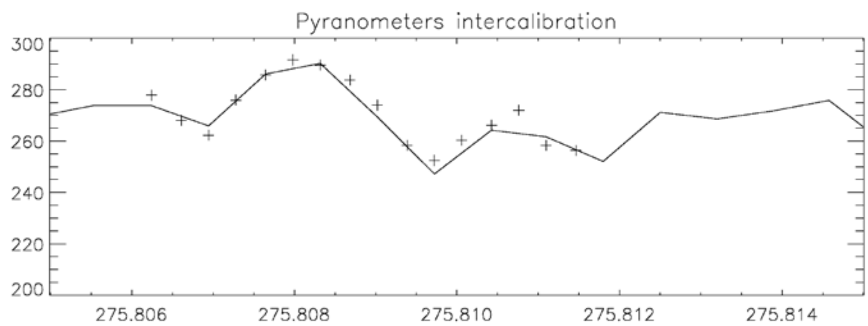

Fig. 6: Incoming SW (W/m²) radiation measured by INSITU (crosses) and SHIP(solid line) pyranometers held side by side on the top of the ship's mast. X values are decimal julian days.

Addressing (2) was only partially resolved. Close to the ship, under cloudy skies, the INSITU radiation is around 10 W/m² higher than measured on the ship. At distance from the ship, under sunny conditions, the INSITU radiation is 10-20 W.m-2 higher than measured on the SHIP. Nevertheless, under cloudy / mixed skies, differences can be either positive or negative depending on the differences in the local sky pattern. In conclusion there is a clear trend toward higher SW fluxes at lower altitude, but this can not be true if there are differences in local sky conditions. The item (3) was evidenced by comparing radiation INSITU at distance from the ship, at Brussels and Liège sites, to SHIP measurements. Significant, but not systematic differences were observed. We attributed them due to differences in the local cloud pattern. In one instance, the Liège site was right downwind the ship. During a sky clearup, the INSITU and SHIP signals were observed to be out of phase with a time-lag of a few minutes. In another instance, in which the station was not downwind the ship, the local sky pattern between Brussels and the ship were different, resulting in net significant differences between both radiometers recordings.

Therefore, if possible, INSITU, rather than SHIP radiation data should be used in a local heat balance computations. High frequency variations in local sky conditions have significant impact on levels of solar irradiance. Since clouds are involved, similar differences in LW radiation are expectable.

4.2 Radiation analysis

Here, we discuss only the SHIP data, without any correction. The SW radiation was on average 124 W/m², and has trend of 3.5 W/m² over the ice station. PAR was 625 µE/m²/s. The LW radiation was on average 227 W/m². As expected, SW and PAR show a marked diurnal cycle, while LW does not.

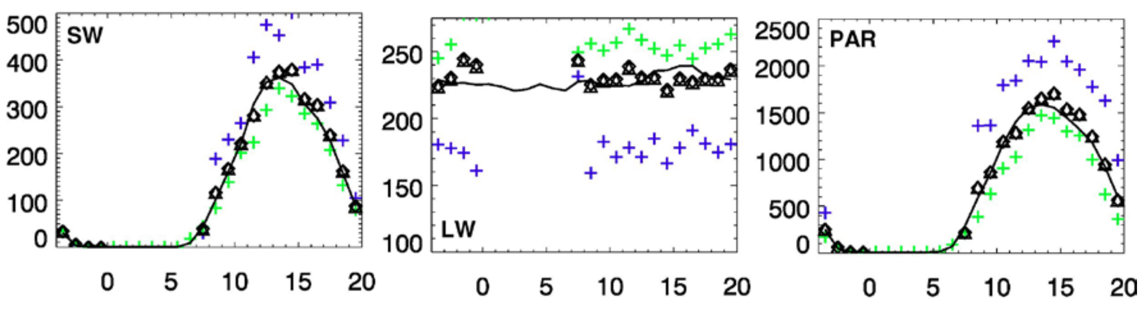

Fig. 7: Radiative fluxes (SW, W/m², left; LW, W/m², center and PAR, µE/m²/s) at Ice station Belgica: All skies (black solid lines), clear skies (blue crosses), and cloud skies (green crosses). Weighted means using the relative number of cloud hours (black diamonds) and cloudiness (black crosses) are shown. Data gaps reflect the lack of visual cloudiness observations during night time.

The variations from the mean of the hourly values of radiative fluxes are governed by the state of the sky. From the VISUAL cloudiness data set, we computed the visual cloudiness binary index C_{iv} (1 if cloudiness is greater than 3 and 0 otherwise). Using C_{iv}, we computed the mean diurnal cycles of radiative fluxes for cloudy skies and overcast skies. From overcast to cloudy skies, the SW flux increase by 50-150 W/m² and LW decreases by 70-100 W/m² between overcast and clear skies. PAR increases by 300-700 µE/m²/s under clear skies.

4.3 Cloudiness reconstructions

Since the sky state has such an impact on radiative fluxes, we tried to see if one could get some information on cloudiness from the radiative fluxes and the answer is yes to a certain extent. We defined the reconstructed cloudiness binary index C_{ir} using hourly anomalies (i.e., the difference between actual hourly values and the value at the corresponding hour from the average diurnal cycle) of radiative fluxes. C_{ir} equals 1 if the hourly anomalies of LW and SW are respectively positive and negative and 0 if not. During the night, only the LW anomalies are used. As expected, C_{ir} and C_{iv} have the same value 87% of the time. Then, we defined the reconstructed daily cloudiness C_r as the daily average number of cloud hours multiplied by ten. Visual cloudiness C_v and C_r are have a correlation coefficient of 0.77. C_v is on average higher than C_r by 0.66. Therefore, cloudiness can be reasonably well reconstructed from hourly recordings of SW and LW radiation, which might be applied to the Ice Mass Balance Buoys. This would be quite useful given the importance of cloudiness on the ice optical properties.

5. In situ measurements

At both Brussels and Liège sites, snow depth and albedo were measured at each visit. Albedo was measured on 6 points, each of them spaced by 5 m on an 25-m long "albedo" line, about 20 m away from the BB sites and on a 7^{th} "albedo" point much closer. Snow depth was measured every meter along the albedo line with a graduated wood stick.

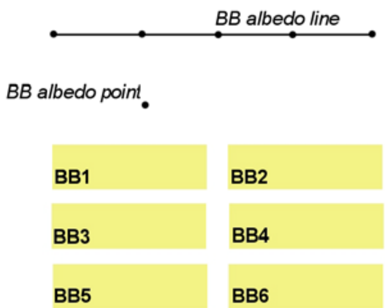

Fig. 8 : Brussels and Liège Sites spatial repartition.

5.1 Snow depth

Considered over all visits, the observed snow depth significantly increased at Brussels sites by 6 cm (mean standard deviation over the line = 5.2 cm). At Liège, the 2.7 cm increase is not significant (mean STD over the line = 12.4 cm). Since snow depth was much higher at Liège from the first station on, the formation of snow-ice might explain the differences. The role of blowing snow should also be considered. This has to be examined in the light of the other measurements.

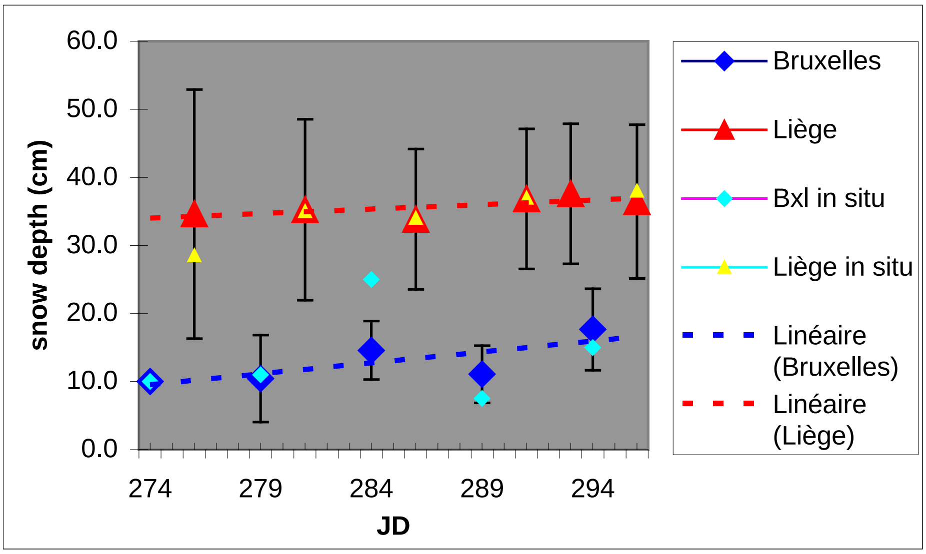

Fig. 9: Average snow depth along the 26 albedo line measurements made at each vist at Brussels (deep blue) and Liège (red). Trends and error bars are also depicted. The small blue diamonds and yellow triangles indicate the point snow measurement made at the BB subsite.

5.2 Albedo

Surface albedo is measured using a bidirectional pyranometer. The tension measured on a multimeter is converted into a values of incoming (F_{in}) and outgoing (F_{out}) SW fluxes. The albedo is given by $\alpha = F_{out}/F_{in}$. Typically, five measurements on a 1-minute time lap were made. On many instances, a picture of the state of the surface was made.

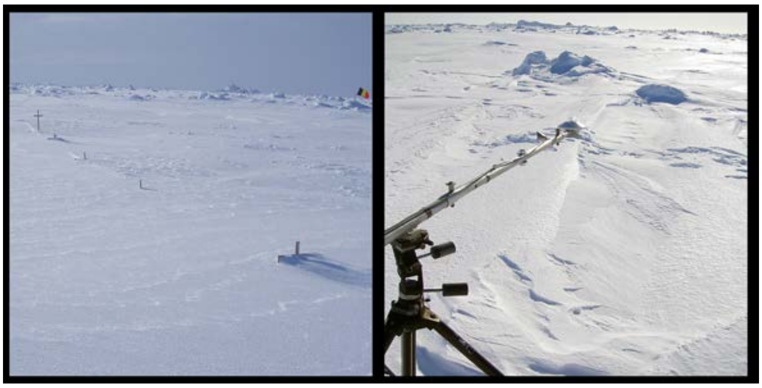

Fig. 10 : (left) The Brussels "Cimetière d'Ixelles" albedo line. (right) Typical position of the pyranometer on the line.

Under cloudy skies, the measurements are easy and do not depend a lot on the leveling of the instrument. Under clear skies, we were very careful to correctly level the instrument to which measurements were found to be quite sensitive. Under mixed skies, measurements are difficult, since the incoming radiation can vary signficantly over very short periods. Measurements were made as close as possible from the solar maximum altitude since the observation error on albedo is higher for a smaller incoming flux.

Observations were performed at WI-1 and at each visit at Brussels and Liège sites. Bad weather prevented albedo measurements to be done at Liège visit #4, therefore a second visit (JD 293) was done two days after. At Liège visit #5, instrument failure after the second albedo line point prevented the measurements to be continued until the end of the line.

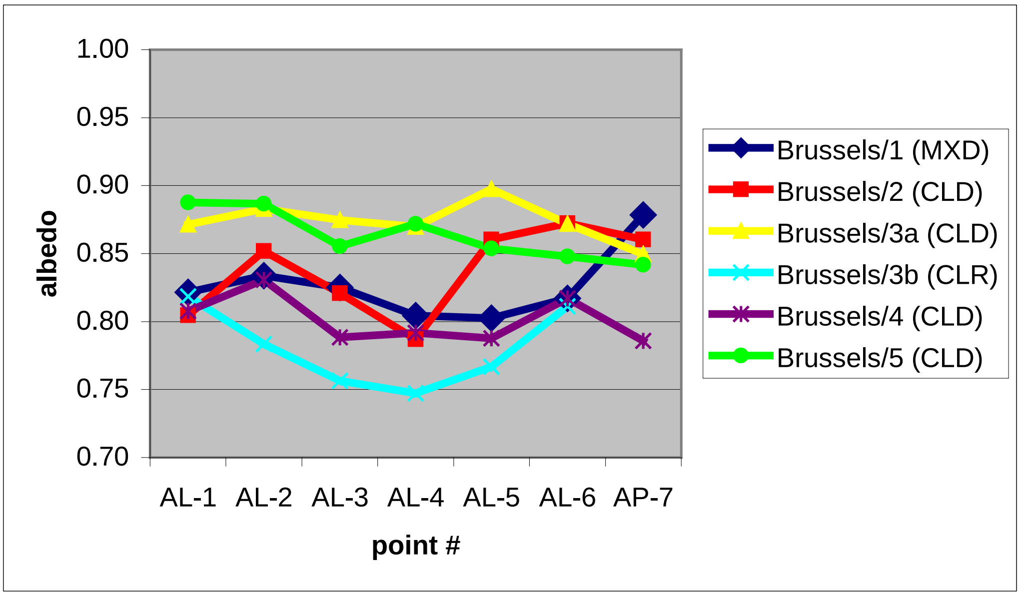

Fig. 11 : Summary of albedo measurements at Brussels. Point #1-6 are on the albedo line and Point #7 is the albedo point. MXD refers to Mixed sky, CLD to cloudy sky and CLR to clear sky.

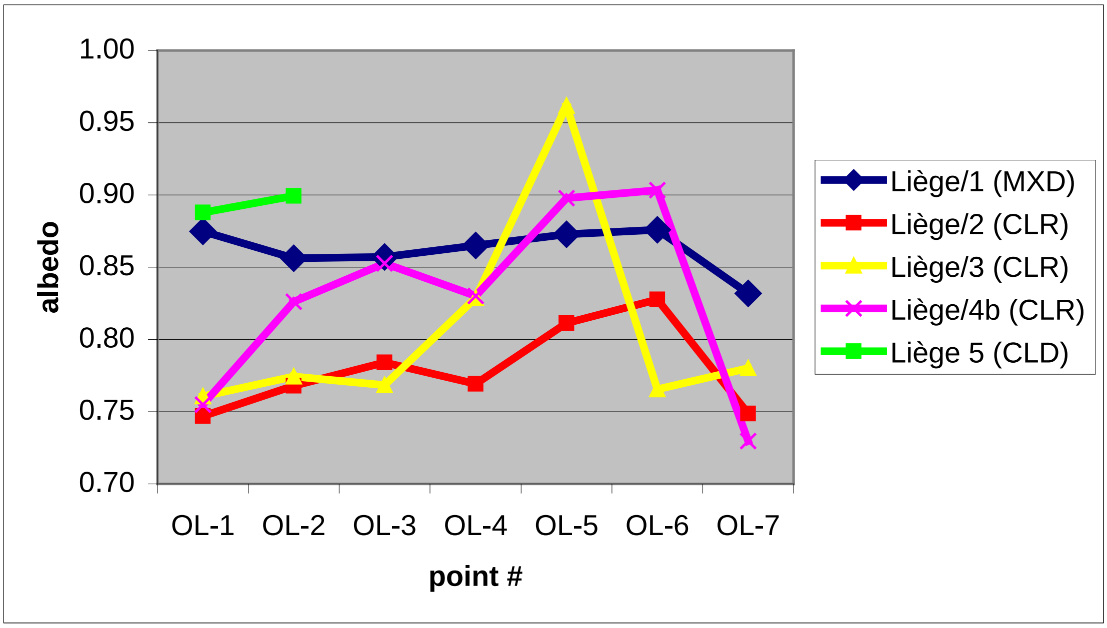

Fig. 12 : Same as Fig.11, but for Liège site

The mean albedo over all measurements is 0.83 ± 0.05. Observations show that variations around this mean value are explained primarily by the nature of the light (diffuse or direct), controlled by the local cloud – clear sky pattern. Cloud-sky albedo is on average higher and less variable (0.85 ± 0.03) than under clear sky (0.81 ± 0.06). Diffuse light has a spectrum which is different from direct light, which in turn affects the large-band, integrated albedo. The passage from diffuse to direct light conditions was observed on two instances and illustrate the albedo transition. The other factors of importance on the variations in surface albedo are snow depth and the “age” of snow.

Almost all Brussels visits were occuring under cloudy sky while Liège visits were under clear sky three times over five. Liège has a slightly higher clould-sky albedo (0.87 ± 0.01) than Brussels (0.84 ± 0.03) because of the snow depth difference. Due to the increase in snow depth, the albedo at Brussels increased from visit #1 (0.83) to visit #3 (0.87). Consistently, if the snow is fresh and deep, the cloud sky albedo is high (0.87). If the snow is old, wind-packed and presents icy layers, the cloud sky albedo is consistently lower (0.80), as shown by observations at Brussels, visit #4. If the snow is thin, as it was the case at visit 1 at Brussels, the albedo is also lower (0.83), close to bare ice (0.80) albedo.

Under clear sky conditions, the measurements show a larger scatter and are more difficult to interpret. There is a tendency for powder, fresh snow to have higher albedo than crusty surfaces, especially if they present large roughness features. Nevertheless, the measurements are not all consistent. Finally, the changing surface conditions due to snowfall and blowing snow, bringing or removing new powder snow, observed in one instance can create significant subdaily albedo variations.

6. Conclusions and perspectives

A series of met, radiation and snow measurements were performed and / or analyzed at Ice Station Belgica. The weather was driven by the wind direction and by the continental or oceanic origin of the air masses. Cloudiness has a tremendous control on the radiative fluxes and on the surface albedo. Measurements along the albedo line show that the snow depths increases at Brussels and remains constant at Liège. Finally, the albedo is 0.83 on average, with variations governed by sky state, snow depth and age.

In the near future, we plan to compute an interpolated time series of ice albedo (using cloudiness reconstructions), to compute the oceanic heat fluxes using the Ice Mass Balance Buoys, and to compute the turbulent surface heat fluxes using a 1-D thermodynamic models run at both sites. The model simulations will also help to give information on the different growth / melt mechanisms to be compared to the ice granulometry data from thin sections and from geophysical observations. In the mid-longer term, both sites data can be used to drive a physical-biogeochemistry model of sea ice. All data will be shared with the SIMBA community.